Journal of Materials Chemistry C

Accepted Manuscript

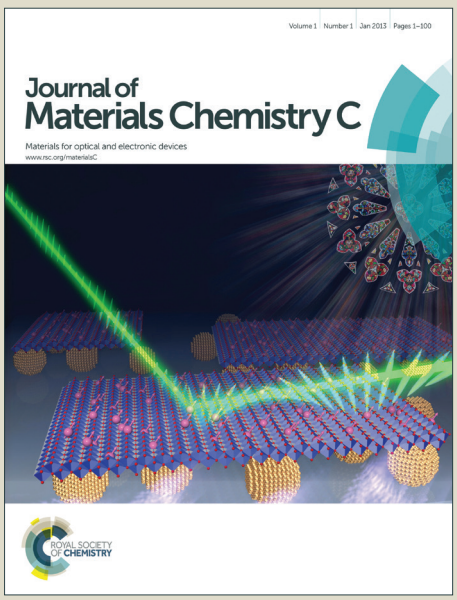

ROYAL SOCIETY OF CHEMISTRY

www.rsc.org/materialsC

Journal Name

RSCPublishing

ARTICLE

Ambipolar Transistor Properties of 2,2′-Binaphthosemiquinones

Cite this: DOI: 10.1039/x0xx00000x

Toshiki Higashino,*[a] Shohei Kumeta,[a] Sumika Tamura,[a] Yoshio Ando,[b] Ken Ohmori,[b] Keisuke Suzuki,[b] and Takehiko Mori*[ac]

Received 00th January 2012,
Accepted 00th January 2012

DOI: 10.1039/x0xx00000x

www.rsc.org/

Binaphthosemiquinones are proved to show ambipolar transistor properties. These compounds have characteristic blue colors owing to the small energy gaps, because the quinone part works as an electron acceptor and the alkoxy group acts as an electron donor. Accordingly, these molecules have an analogous electronic structure to indigo. The crystal structure changes depending on the alkoxy groups, though these compounds generally have stacking structures.

Introduction

In recent years, growing interests have been devoted to ambipolar semiconductors because of the potential application to large-area integrated circuits, light-emitting transistors, and photovoltaic devices.[1] Among them, donor-acceptor (D-A) copolymers composed of electron-rich and electron-deficient units have been investigated intensively owing to the high performance and well-balanced ambipolar charge transport in organic transistors.[2] In particular, D-A copolymers composed of diketopyrrolopyrrole (DPP) and thiophene derivatives exhibit excellent ambipolar characteristics due to the remarkable aggregation properties,[3] where DPP works as the acceptor part. As another acceptor unit, isoindigo has been investigated recently,[4] and indigo has been also used in an ambipolar D-A copolymer.[5] These ambipolar D-A copolymers have a small band gap between the highest occupied molecular orbital (HOMO) and the lowest unoccupied molecular orbital (LUMO) levels, which is important for the effective hole and electron injection from a single electrode material.

It has been recently found, however, that the component small molecule, indigo, exhibits ambipolar transistor properties.[6] In particular, dibromo and diphenyl indigo exhibit much improved ambipolar transistor properties in the order of 0.1 - 1 $cm^2 V^{-1} s^{-1}$. This demonstrates that indigo itself is an ambipolar material with a small HOMO-LUMO gap, and this is quite convincing because the characteristic deep blue color with the absorption edge around 720 nm is related to the small HOMO-LUMO gap of 1.7 eV. The possibility of ambipolar transport has been also suggested from the molecular orbital calculation not only for indigo but also for isoindigo and DPP.[7]

In general, aromatic compounds with a deep violet color are candidates of ambipolar semiconductors. In this connection, 2,2′-binaphthosemiquinones (BNQs, Scheme 1) have a characteristic blue color, which has been known as Russing blue for a long time.[8] Since the NH moiety in indigo is an electron donating group and has two π electrons, the C=C unit with the alkoxy part in BNQ works analogously to the NH group. Here we investigate electronic and crystal structures as well as the transistor properties of BNQs with various alkyl groups (Scheme 1).

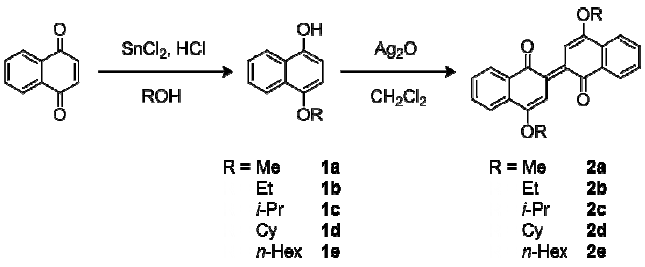

Scheme 1. Synthesis of BNQ derivatives

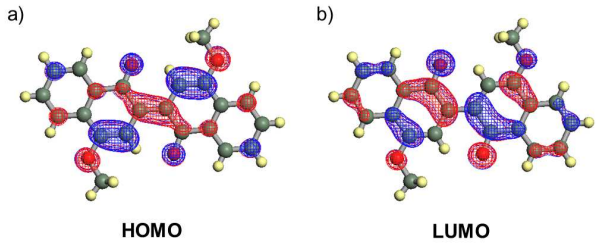

Fig. 1 Molecular orbitals of **2a**: (a) HOMO and (b) LUMO.

Table 1 Redox potentials for BNQ derivatives (vs. Fc/Fc^+ coupling = –4.80 eV).

	E_{onset}^{Ox} (V)	E_{onset}^{Red} (V)	E_{HOMO} (eV)	E_{LUMO} (eV)	ΔE^{CV} (eV)	ΔE^{opt} (eV)
2a	0.48	–1.00	–5.28	–3.80	1.48	1.75
2b	0.45	–1.01	–5.25	–3.79	1.46	1.73
2c	0.42	–1.02	–5.22	–3.78	1.44	1.69
2e	0.41	–1.03	–5.21	–3.77	1.44	1.68
2d	0.47	–1.02	–5.27	–3.78	1.49	1.72

Results and discussion

Synthesis

The synthesis of BNQ derivatives **2a-e** is outlined in Scheme 1. 1,4-Naphthoquinone was reduced to 4-alkoxy-1-naphthols **1a-e** in the presence of the corresponding alcohols by treatment with tin(II)chloride and concentrated hydrogen chloride under reflux for 3 hours in 42-64% yields.[9] The obtained 4-alkoxy-1-naphthols **1a-e** were oxidized with silver (II)oxide in chloroform at room temperature for 3 hours to give the corresponding BNQ derivatives **2a-e** in 40-83% yields. All BNQ derivatives are highly soluble in halogenated solvents, and stable in the solid form.

Elecrtochemical properties

The electrochemical properties were studied by cyclic voltammetry (Figure S1). All compounds showed two quasi-reversible reduction waves and one quasi-reversible oxidation wave, from which the HOMO and LUMO energy levels were estimated as shown in Table 1. The HOMO level is about –5.3 eV and the LUMO level is –3.8 eV, and the resulting energy gap is as narrow as 1.5 eV. This is attributed to the semiquinone structure, suggesting the capability of these compounds for both electron and hole transport. A general rule has been suggested that hole transport is realized for Au electrodes when the HOMO is located above –5.6 eV, and electron transport is achieved when the LUMO level is located deeper than –3.15 eV.[10] The estimated HOMO/LUMO levels of the present compounds satisfy these conditions.

These energy level values do not conflict with the results of the density functional theory (DFT) calculations by Gaussian 09 program at the level of B3LYP using the 6-31G(d,p) basis set (HOMO : –5.05 eV and LUMO : –2.89 eV for **2a**).[11] As shown in Figure 1, the DFT calculation demonstrates characteristic electron distribution of the HOMO and LUMO on the semiquinone backbone; there is a large LUMO population centered on the carbonyl carbons, whereas the HOMO population is localized around the alkoxy carbons. Therefore, naively speaking, the carbonyl groups act as the electron

Table 2 Crystallographic data for **2a-e**.

Crystals	**2a**	**2b**	**2c**	**2d**	**2e** [12]
Empirical formula	$C_{22}H_{16}O_4$	$C_{24}H_{20}O_4$	$C_{26}H_{24}O_4$	$C_{32}H_{32}O_4$	$C_{32}H_{36}O_4$
Formula weight	344.37	372.42	400.47	480.58	484.61
Crystal system	Orthorhombic	Monoclinic	Monoclinic	Monoclinic	Triclinic
Space group	$P2_12_12_1$	$P2_1/n$	$C2/c$	$C2/c$	P-1
a (Å)	4.5570(5)	12.2447(3)	29.3578(7)	23.0134(5)	5.3199(3)
b (A)	18.571(2)	4.98276(9)	4.3053(2)	16.3860(3)	10.5254(6)
c (Å)	18.986(3)	15.1193(3)	18.6433(5)	15.4408(3)	12.2657(9)
α (°)	90	90	90	90	71.587(6)
β (°)	90	93.255(1)	118.437(2)	119.5322(9)	82.118(5)
γ (°)	90	90	90	90	75.890(5)
V (Å^3)	1606.8(3)	920.97(3)	2072.1(1)	5066.2(2)	630.63(7)
Z	4	2	4	8	1
Unique reflns. (R_{int})	2948 (0.0933)	1664 (0.1752)	1866 (0.0357)	4599 (0.0311)	2346 (0.0369)
D_{cal} (g/cm^3)	1.423	1.343	1.284	1.255	1.276
R_1	0.0859	0.0638	0.0413	0.0419	0.0414
R_w	0.1917	0.1527	0.0904	0.1020	0.1138
GOF	1.089	1.012	1.024	1.240	0.964

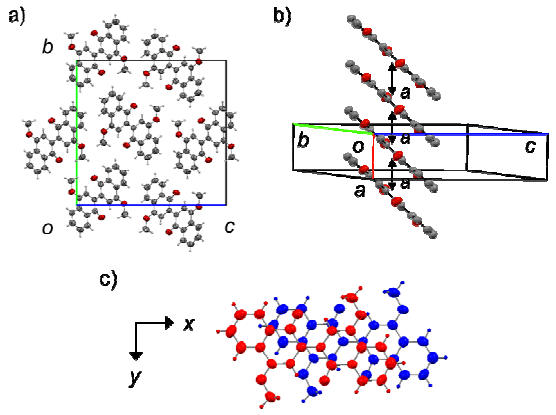

Fig. 2 Crystal structures of **2a**, viewed along (a) the stacking direction and (b) the molecular short axis, and (c) the overlap modes.

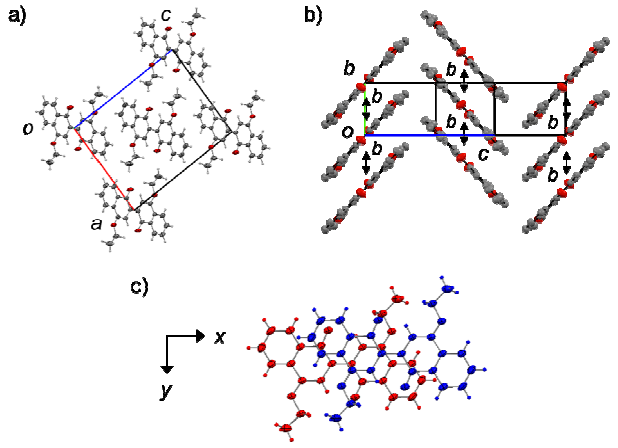

Fig. 3 Crystal structures of **2b**, viewed along (a) the stacking direction and (b) the molecular short axis, and (c) the overlap modes.

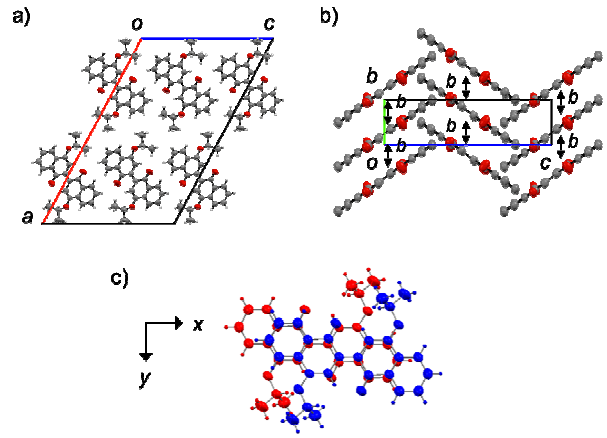

Fig. 4 Crystal structures of **2c**, viewed along (a) the stacking direction and (b) the molecular short axis, and (c) the overlap modes.

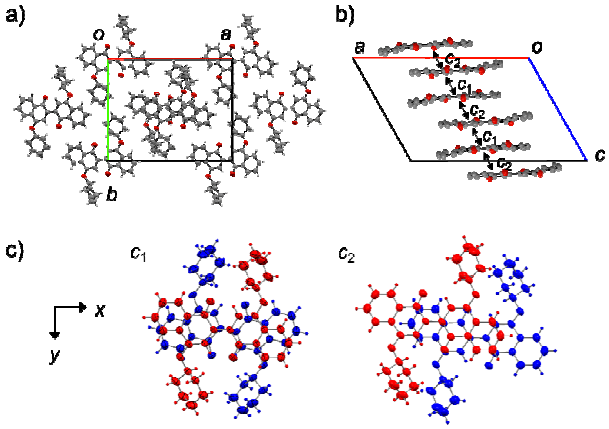

Fig. 5 Crystal structures of **2d**, viewed along (a) the stacking direction and (b) the molecular short axis, and (c) the overlap modes.

acceptors and the alkoxy groups as the electron donors. This is analogous to indigo having the large LUMO population on the carbonyl groups, and the HOMO population on the amino groups.[12]

Crystal structures

Needle-like black crystals of the BNQ derivatives **2a-e** were obtained by recrystallization from toluene. Single crystal X-ray structure analyses were carried out for **2a**, **2b**, **2c**, and **2d**. Table 1 shows the crystallographic data together with the reported data of **2e**.[13] These compounds have respectively different crystal structures.

A crystal of **2a** belongs to an orthorhombic system with the space group $P2_12_12_1$. The crystal packing is depicted in Figure 2. One molecule is crystallographically independent, and the unit cell contains four molecules, which are related to each other by a 2_1-screw axis running along the three different crystallographic axes. The molecule is almost planar, and forms a one-dimensional uniform stack along the *a*-axis with the interplanar spacing of 3.36 Å (Table 3). On account of the screw axes, the long axes of the molecules in the adjacent stacks are not parallel, and oriented alternately.

A crystal of **2b** belongs to a monoclinic system with the space group $P2_1/n$, where the crystal packing is depicted in Figure 3. The crystallographically independent unit consists of half the molecule, and the unit cell contains two molecules. The molecule is almost planar, and forms a one-dimensional uniform stack along the *b* axis. All molecular long axes are oriented parallel in the *ac* plane, but tilted alternately, so that when viewed from the molecular short axis, the structure looks like the herringbone structure (Fig. 3(b)).

A crystal of **2c** belongs to the space group *C*2/*c*, where the crystal packing is depicted in Figure 4. Half the molecule is crystallographically independent, and a unit cell contains four molecules. Similarly to **2b**, the planar molecules form a one-dimensional uniform stack along the *b*-axis, where the side view from the molecular short axis looks like the herringbone-like packing as well.

A crystal of **2d** belongs to a monoclinic system with the space group *C*2/*c*, where the crystal packing is depicted in Figure 5. The unit cell contains eight molecules, and one

Table 3 Transfer integrals and geometries of **2a-e**.

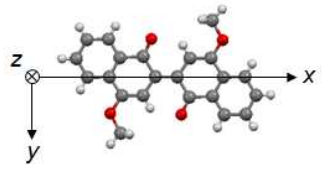

Definition of molecular coordinates

	mode	t_{HOMO} (meV)	t_{LUMO} (meV)	x (Å)	y (Å)	z (Å)
2a	a	–59	–35	3.06	0.36	3.36
2b	b	–58	51	3.66	0.68	3.32
2c	b	11	–54	2.27	0.89	3.55
2d	c_1	27	30	0.52	0.19	3.37
	c_2	8	–46	3.78	0.75	3.63
2e	a	–32	87	4.03	0.94	3.34

molecule is crystallographically independent. The molecule is not perfectly planar, and the two naphthyl parts make an angle of 14.2° due to the large steric hindrance of the cyclohexyl groups. The molecules are dimerized along the *c*-axis stack, forming a one-dimensional column with two kinds of π-π overlaps,

In contrast to indigo, BNQ does not form strong intercolumnar N–H···O hydrogen bonds because the donor part is replaced by an alkoxy group; this is probably associated with the thin needle-like shape of the BNQ crystals. However, there are many intermolecular C–H···O hydrogen bonds using alkyl and aromatic hydrogens, where the typical distance from the carbonyl O to the alkyl C is 3.18 ~ 3.43 Å.[14] Compound **2a** has an additional hydrogen bond using the alkoxy O···C, 3.56 Å. Compound **2b** is stabilized by the hydrogen bond network using two carbonyl O atoms and two alkoxy O atoms (O···C: 3.44 Å), which indicates the relatively dense packing of **2b**.[7a,15]

The present BNQ compounds (**2a-c**) are entirely planar due to the central C=C double bond. On the other hand, the corresponding oxidized quinone, 2,2′-bi-1,4-naphthoquinone, has a twisted structure; at the central C2-C2′ single bond the aromatic planes are twisted with the torsion angle of 47.3°.[16] The resulting intramolecular O···H distance is 2.54 Å, which is considerably longer than 2.05 Å in the present compounds.

Overlap modes and transfer integrals

In order to compare the intermolecular interaction more carefully, the geometries of the BNQ molecules in the stack are compared in Table 3 together with the intermolecular HOMO-HOMO and LUMO-LUMO transfer integrals. The respective overlap modes are depicted in Figure 2(c), 3(c), 4(c), and 5(c). Here, the direction of the central C=C double bond is defined as the *x* axis (Table 3), and its vertical direction in the molecular plane is taken as the *y* axis. Then the position of the adjacent molecule in the stack is represented by the (*x*, *y*, *z*) coordinates. Accordingly, the *z* component means the interplanar distance.

In **2a** and **2b**, the *y* displacement is comparatively small ($y <$ 0.7 Å), and the stacked molecules are slipped mainly along the *x* axis, namely parallel to the central C=C bond. Since the *x* displacement is around 3.0 ~ 3.7 Å, the stacking mode looks like a ring-over-bond type (Figure 2(c) and 3(c)). These compounds have short interplanar distances (*z* displacement) of 3.36 Å and 3.32 Å, and comparatively large transfer integrals. By contrast, **2c** has a nearly eclipsed stacking mode (Figure 4(c)), and as a result, the interplanar distance is slightly large (3.55 Å). Compound **2d** has a dimerized structure, where the geometry c_2 is not much different from those of **2a** and **2b**, though the interplanar distance is somewhat large (3.63 Å). In c_1, the molecular long axes are no more parallel but connected

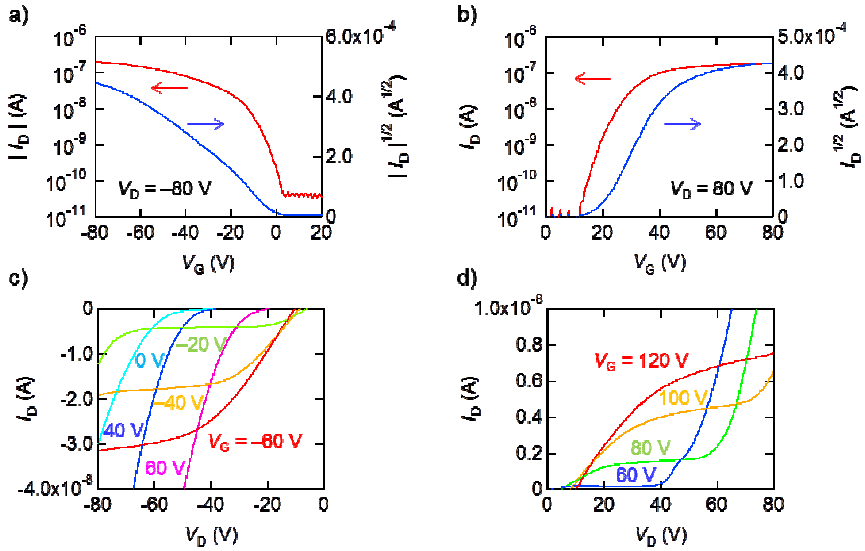

Fig. 6 Characteristics of the ambipolar transistors based on **2b** deposited on TTC. (a) Transfer characteristics in the p-channel region, and (b) the n-channel region. (c) Output characteristics in the p-channel region, and (d) the n-channel region.

Table 4 Transistor characteristics for **2a-c**.

		μ^{ave} [μ^{max}] ($cm^2\ V^{-1}\ s^{-1}$)	V_{th}^{ave} (V)	on/off^{ave}
2a	h	8.2×10^{-4} [1.8×10^{-3}]	–1.5	4×10^4
	e	7.0×10^{-4} [1.2×10^{-3}]	29	4×10^3
2b	h	1.3×10^{-3} [3.6×10^{-3}]	–0.1	1×10^4
	e	4.7×10^{-3} [6.2×10^{-3}]	10	1×10^4
2c	h	5.7×10^{-4} [1.1×10^{-3}]	–2	5×10^3
	e	1.2×10^{-4} [2.5×10^{-4}]	30	1×10^3

by a two-fold axis (Figure 5(c)), where the small x and y displacements imply that the molecular center is placed approximately on the top of the other molecule. The considerable dimerization is also obvious from the calculated transfer integrals. The geometry of **2e** is in principle not much different from those of **2a** and **2b**, though the x and y displacements are somewhat enlarged. There is a general tendency that large alkyl groups reduce the intermolecular overlap. The large transfer integrals are observed only in the stacking direction, and there are no meaningful intercolumnar transfer integrals. These compounds have highly one-dimensional electronic structures, though the resulting bandwidths are not very small (~0.2 eV). The signs of the transfer integrals change depending on the compounds (Table 3), because the intermolecular overlap modes are respectively different.

Transistor properties

In order to investigate charge-carrier transport in BNQ derivatives, the organic thin-film transistors were fabricated. Tetratetracontane ($C_{44}H_{90}$, TTC) was evaporated on the thermally grown silicon oxide layer of an n-type silicon wafer. TTC is a highly hydrophobic material with a small dielectric constant, and recently proved to be an excellent passivation layer to observe ambipolar transport.[6] Compounds **2a**, **2b**, and **2c** were vacuum evaporated. Then, gold source-drain electrodes were evaporated on the active layer, and the resulting bottom-gate top-contact devices were investigated under vacuum and ambient conditions. We could not obtain evaporated films of **2d** and **2e**. Transistors of spin-coated films of these compounds were investigated, but not successfully operated.

The transfer and output characteristics of the **2b** device are shown in Figure 6, and the extracted parameters are listed in Table 4 together with the results of **2a** and **2c**. The device exhibits typical ambipolar behavior; it can be operated both at negative and positive gate voltages (V_G). The hole and electron transporting properties are well balanced, with the hole and electron average mobilities around 1.3×10^{-3} $cm^2\ V^{-1}\ s^{-1}$ and 4.7×10^{-3} $cm^2\ V^{-1}\ s^{-1}$, respectively. The balanced performance does not conflict with the balanced transfer integrals estimated from the crystal packing (Table 3). Although the mobility values are moderate, we have achieved large on/off ratios exceeding 10^4 (Table 4). In addition, the ambipolar regions are clearly observed in the output characteristics (Figures 6(c) and (d)). This is represented by the comparatively small threshold voltages V_{th} (Table 4). The threshold voltages are also estimated from the rise of the reversed current in the output characteristics according to $V_T' = V_G - V_D$, which are in good agreement with the estimations from the transfer characteristics.[6d,17] The transistor of **2b** shows ambipolar performance even under ambient conditions and after several-months storage under air (Figure S3). Compounds **2a** and **2c** show slightly smaller mobilities, and the hole transport is larger than the electron transport (Figure S4 and S5); the hole current is obviously by one order of magnitude larger than the electron current. In view of the energy levels (Table 1), the hole transport is to some extent preferable to the electron transport in these materials. The decreasing order of mobility **2b** > **2a** > **2c** roughly coincides with the increasing order of the interplanar distances (Table 3), and the mobility is related to the preferable molecular packing. However, the generally small mobility is ascribable to the one-dimensional structure, where the charge transport is restricted in the stacking direction.

Thin film properties

Figure 7 shows the X-ray diffraction (XRD) patterns and the AFM topographical images. AFM images show polycrystalline thin films composed of needle-like grains of several micrometers, indicating the one-dimensional pathway along the elongated axis. The XRD patterns show a broad peak centered at about 4.4° (d-spacing = 20 Å) corresponding to the (006) reflection of the orientated TTC film.[18] The primary thin-

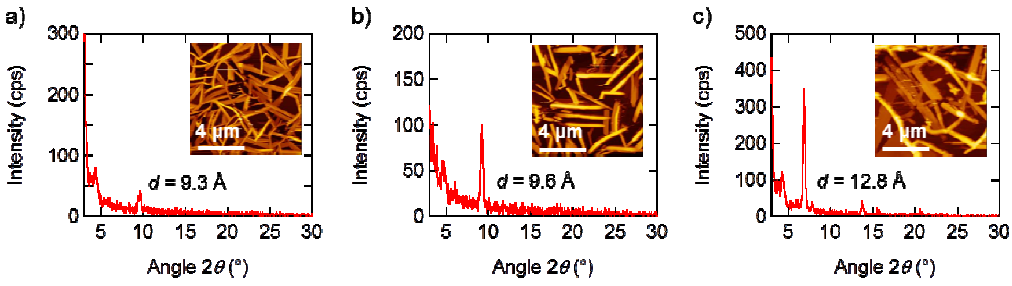

Fig. 7 X-ray diffraction patterns and AFM topographical images of 40 nm BNQ thin-films deposited on TTC: (a) **2a**, (b) **2b**, and (c) **2c**.

film *d*-spacings of **2a-c** are estimated to be 9.2 Å for **2a**, 9.5 Å for **2b**, and 12.7 Å for **2c**. These *d*-spacings respectively correspond to $\boldsymbol{b}/2$, $(\boldsymbol{a} - \boldsymbol{c})/2$, and $(\boldsymbol{a} \sin \beta)/2$ of the crystal lattice, indicating that the alkyl chains are standing perpendicular to the substrate for **2b** and **2c** with keeping the molecular layers parallel to the substrate. From this, the molecular planes are tilted from the substrate normal by 13° for **2a**, 5° for **2b**, and 18° for **2c**. The molecules of **2b** are aligned most closely to the vertical direction of the substrate. It has been demonstrated that the charge mobility is maximized when the molecules are exactly perpendicular to the substrate, and decreases as the tilt angle increases.[19] This rule is valid in the present compounds.

Conclusions

Binaphthosemiquinones are proved to show ambipolar transistor properties. These compounds have one-dimensional stacks, and because the charge transport is restricted in the stacking direction, the hole and electron mobilities are in the order of 10^{-3} cm^2 V^{-1} s^{-1}. In general, there is a tendency that a bulky alkyl group reduces the intermolecular overlap and charge transport properties. The ambipolar properties are obviously associated with the small HOMO-LUMO gaps and the characteristic blue colors. Such a property comes from the semiquinone structure. The quinone parts work as an electron acceptor and the alkoxy groups act as an electron donor, and these molecules contain donor and acceptor parts in a molecule. The present work demonstrates retrospectively that indigo is, in a sense, regarded as a modified semiquinone. These molecules are certainly of interest as a component of organic electronic materials such as donor-acceptor polymers, but it is also of interest how a small HOMO-LUMO gap is realized in a small molecule with a minimal structure.

Acknowledgements

The authors would like to express sincere gratitude to Center for Advanced Materials Analysis, Tokyo Institute of Technology, for X-ray diffraction measurements. This work was partly supported by a Grant-in Aid for Scientific Research (B) (No. 23350061) from the Ministry of Education, Culture, Sports, Science, and Technology of Japan.

Notes and references

[a] Department of Organic and Polymeric Materials, Tokyo Institute of Technology, O-okayama, Meguro-ku, Tokyo, 152-8552, Japan.
[b] Department of Chemistry, Tokyo Institute of Technology, 2-12-1 O-okayama, Meguro-ku, Tokyo 152-8551, Japan.
[c] ACT-C, JST, Honcho, Kawaguchi, Saitama 332-0012, Japan.
E-mail: higashino.t.aa@m.titech.ac.jp, mori.t.ae@m.titech.ac.jp

† Electronic supporting information (ESI) available: CCDC 1031323-1031326 contain the supplementary crystallographic information for **2a-d**. Additional information for synthesis, redox and optical properties, crystal structures, band calcutions, devive fabrication, and thin film properties.

1 (a) M. Muccini, *Nat. Mater.*, 2006, **5**, 605; (b) J. Zaumseil and H. Sirringhaus, *Chem. Rev.*, 2007, **107**, 1296; (c) F. Cicoira and C. Santato, *Adv. Funct. Mater.*, 2007, **17**, 3421; (d) K.-J. Baeg , M. Caironi and Y.-Y. Noh, *Adv. Mater.*, 2013, **25**, 4210. (e) S. Hotta, T. Yamao, S. Z. Bisri, T. Takenobu and Y. Iwasa, *J. Mater. Chem. C*, 2014, **2**, 965; (f) Y. Wakayama, R. Hayakawa and H.-S. Seo, *Sci. Technol. Adv. Mater.*, 2014, **15**, 024202.

2 (a) J. D. Yuen, R. Kumar, D. Zakhidov, J. Seifter, B. Lim, A. J. Heeger and F. Wudl, *Adv. Mater.*, 2011, **23**, 3780; (b) K.-J. Baeg, J. Kim, D Khim, M. Caironi, D.-Y. Kim, I.-K. You, J. R. Quinn, A. Facchetti, and Y.-Y. Noh, *ACS Appl. Mater. Inter.*, 2011, **3**, 3205; (c) J. Fan, J. D. Yuen, M. Wang, J. Seifter, J.-H. Seo, A. R. Mohebbi, D. Zakhidov, A. Heeger and F. Wudl, *Adv. Mater.*, 2012, **24**, 2186; (d) H. Usta, C. Newman, Z. Chen and A. Facchetti, *Adv. Mater.*, 2012, **24**, 3678; (e) K.-J. Baeg, D. Khim, S.-W. Jung, M. Kang, I.-K. You, D.-Y. Kim, A. Facchetti and Y.-Y. Noh, *Adv. Mater.*, 2012, **24**, 5433; (f) J. Kim, K.-J. Baeg, D. Khim, D. T. James, J.-S. Kim, B. Lim, J.-M. Yun, H.-G. Jeong, P. S. K. Amegadze, Y.-Y. Noh and D.-Y. Kim, *Chem. Mater.*, 2013, **25**, 1572; (g) T. Lei, J.-H. Dou, X.-Y. Cao, J.-Y. Wang and J. Pei, *Adv. Mater.*, 2013, **25**, 6589; (h) J. W. Rumer, M. Levick, S.-Y. Dai, S. Rossbauer, Z. Huang, L. Biniek, T. D. Anthopoulos, J. R. Durrant, D. J. Procterb and I. McCullocha, *Chem. Commun.*, 2013, **49**, 4465; (i) H. Chen, Y. Guo, Z. Mao, G. Yu, J. Huang, Y. Zhao and Y. Liu, *Chem. Mater.*, 2013, **25**, 3589; (j) C. Guo, B. Sun, J. Quinn, Z. Yan and Y. Li, *J. Mater. Chem. C*, 2014, **2**, 4289, (k) T. T. Steckler, P. Henriksson, S. Mollinger, A. Lundin, A. Salleo and M. R. Andersson, *J. Am. Chem. Soc.*, 2014, **136**, 1190.

3 (a) J. D. Yuen, J. Fan, J. Seifter, B. Lim, R. Hufschmid, A. J. Heeger and F. Wudl, *J. Am. Chem. Soc.*, 2011, **133**, 20799; (b) J. Lee, A.-R. Han, J. Kim, Y. Kim, J. H. Oh and C. Yang, *J. Am. Chem. Soc.*, 2012, **134**, 20713; (c) T.-J. Ha, P. Sonar, S. P. Singh and A. Dodabalapur, *IEEE Trans. Electron Dev.*, 2012, **59**, 1494; (d) Z. Chen, M. J. Lee, R. S. Ashraf, Y. Gu, S. Albert-Seifried, M. M. Nielsen, B. Schroeder, T. D. Anthopoulos, M. Heeney, I. McCulloch and H. Sirringhaus, *Adv. Mater.*, 2012, **24**, 647; (e) J. Lee, A.-R. Han, H. Yu, T. J. Shin, C. Yang and J. H. Oh, *J. Am. Chem. Soc.*, 2013, **135**, 9540; (f) B. Sun, W. Hong, Z. Yan, H. Aziz and Y. Li, *Adv. Mater.*, 2014, **26**, 2636.

4 (a) T. Lei, J.-H. Dou, Z.-J. Ma, C.-H. Yao, C.-J. Liu, J.-Y. Wang and J. Pei, *J. Am. Chem. Soc.*, 2012, **134**, 20025; (b) T. Lei, J.-H. Dou, Z.-J. Ma, C.-J. Liu, J.-Y. Wang and J. Pei, *Chem. Sci.*, 2013, **4**, 2447; (c) L. A. Estrada, R. Stalder, K. A. Abboud, C. Risko, J.-L. Bredas and J. R. Reynolds, *Macromolecules*, 2013, **46**, 8832.

5 C. Guo, B. Sun, J. Quinn, Z. Yan and Y. Li, *J. Mater. Chem. C*, 2014, **2**, 4289.

6 (a) M. Irimia-Vladu, E. D. Głowacki, P. A. Troshin, G. Schwabegger, L. Leonat, D. K. Susarova, O. Krystal, M. Ullah, Y. Kanbur, M. A. Bodea, V. F. Razumov, H. Sitter, S. Bauer and N. S. Sariciftci, *Adv. Mater.*, 2012, **24**, 375;

(b) Y. Kanbur, M. Irimia-Vladu, E. D. Głowacki, G. Voss, M. Baumgartner, G. Schwabegger, L. Leonat, M. Ullah, H. Sarica, S. Erten-Ela, R. Schwödiauer, H. Sitter, Z. Küçükyavuz, S. Bauer and N. S. Sariciftci, *Org. Electron.*, 2012, **13**, 919; (c) E. D. Głowacki, D. H. Apaydin, Z. Bozkurt, U. Monkowius, K. Demirak, E. Tordin, M. Himmelsbach, C. Schwarzinger, M. Burian, R. T. Lechner, N. Demitri, G. Vossa and N. S. Sariciftci, *J. Mater. Chem. C*, 2014, **2**, 8089; (d) O. Pitayatanakul, T. Higashino, T. Kadoya, M. Tanaka, H. Kojima, M. Ashizawa, T. Kawamoto, H. Matsumoto, K. Ishikawa and T. Mori, *J. Mater. Chem. C*, 2014, **2**, 9311.

7 H. Kojima and T. Mori, *Chem. Lett*., 2013, **42**, 68.

8 (a) D. Schulte-Frohlinde and F. Erhardt, *Liebigs Ann. Chem.*, 1963, 92; (b) H. Laatsch, *Liebigs Ann. Chem.*, 1984, 1367; (c) H. Laatsch, *Liebigs Ann. Chem.*, 1990, 433; (d) C. Göltner and H. Laatsch, *Liebigs Ann. Chem.*, 1991, 1085.

9 T. N. Van, B. Kesteleyn and N. D. Kimpe, *Tetrahedron,* 2001, **57**, 4213.

10 M. L. Tang, A. D. Reicharrdt, P. Wei, and Z. Bao, *J. Am. Chem. Soc*., 2009, **131**, 5264.

11 M. J. Frisch, G. W. Trucks, H. B. Schlegel, G. E. Scuseria, M. A. Robb, J. R. Cheeseman, G. Scalmani, V. Barone, B. Mennucci, G. A. Petersson, H. Nakatsuji, M. Caricato, X. Li,H. P. Hratchian, A. F. Izmaylov, J. Bloino, G. Zheng, J. L. Sonnenberg, M. Hada, M. Ehara, K. Toyota, R. Fukuda, J. Hasegawa, M. Ishida, T. Nakajima, Y. Honda, O. Kitao, H. Nakai, T. Vreven, J. A. Montgomery, Jr., J. E. Peralta, F. Ogliaro, M. Bearpark, J. J. Heyd, E. Brothers, K. N. Kudin, V. N. Staroverov, R. Kobayashi, J. Normand, K. Raghavachari, A. Rendell, J. C. Burant, S. S. Iyengar, J. Tomasi, M. Cossi, N. Rega, J. M. Millam, M. Klene, J. E. Knox, J. B. Cross, V. Bakken, C. Adamo, J. Jaramillo, R. Gomperts, R. E. Stratmann, O. Yazyev, A. J. Austin, R. Cammi, C. Pomelli, J. W. Ochterski, R. L. Martin, K. Morokuma, V. G. Zakrzewski, G. A. Voth, P. Salvador, J. J. Dannenberg, S. Dapprich, A. D. Daniels, O. Farkas, J. B. Foresman, J. V. Ortiz, J. Cioslowski, D. J. Fox, Gaussian 09 (Revision B. 01), Gaussian, Inc., Wallingford CT, 2009.

12 (a) H. Bauer, K. Kowski, H. Kuhn, W. Lüttke and P. Rademacher, *J. Mol. Struct.*, 1998, **445**, 277; (b) L. Serrano-Andrés and B. O. Roos, *Chem. Eur. J.*, 1997, **3**, 717.

13 A. N. Cammidge, V. H. M. Goddard, C. P. J. Schubert, H. Gopee, D. L. Hughes and D. G-. Lucas, *Org. Lett.*, 2011, **13**, 6034.

14 J. R. Desiraju, *Acc. Chem. Res.*, 1991, **24**, 290.

15 H. Yanagisawa, J. Mizuguchi, S. Aramaki and Y. Sakai, *Jpn. J. Appl. Phys.*, 2008, **47**, 4728.

16 H. L. Ammon, M. Sundaralingam and J. M. Stewart, *Acta. Cryst. B*, 1969, **25**, 336.

17 T. Higashino, J. Cho and T. Mori, *Appl. Phys. Express*, 2014, **7**, 121602.

18 J.-P. Gorce, S. J. Spells, X.-B. Zeng and G. Ungar, *J. Phys Chem B*, 2004, **108**, 3130.

19 T. Kakinuma, H. Kojima, M. Ashizawa, H. Matsumoto and T. Mori, *J. Mater. Chem. C*, 2013, **1**, 5395.

The table of contents entry

Title
Ambipolar Transistor Properties of 2,2′-Binaphthosemiquinones

Text (one sentence, of maximum 20 words, highlighting the novelty of the work)
Binaphthosemiquinones having characteristic blue colors owing to the small energy gaps are proved to show ambipolar transistor properties.

Keywords
organic transistor, organic semiconductor, ambipolar transport, donor-acceptor

Authors
Toshiki Higashino, Shohei Kumeta, Sumika Tamura, Yoshio Ando, Ken Ohmori, Keisuke Suzuki, and Takehiko Mori

ToC figure (maximum size 8 cm x 4 cm)